Noise analysis and measurement of time delay and integration charge coupled device*

Wang De-Jiang(王德江)[a)b)†] and Zhang Tao(张 涛)[a)]

[a)]*Changchun Institute of Optics, Fine Mechanics and Physics, Chinese Academy of Sciences, Changchun* 130033, *China*
[b)]*Graduate School of the Chinese Academy of Sciences, Beijing* 100049, *China*

Time delay and integration (TDI) charge coupled device (CCD) noise sets a fundamental limit on image sensor performance, especially under low illumination in remote sensing applications. After introducing the complete sources of CCD noise, we study the effects of TDI operation mode on noise, and the relationship between different types of noise and number of the TDI stage. Then we propose a new technique to identify and measure sources of TDI CCD noise employing mathematical statistics theory, where theoretical analysis shows that noise estimated formulation converges well. Finally, we establish a testing platform to carry out experiments, and a standard TDI CCD is calibrated by using the proposed method. The experimental results show that the noise analysis and measurement methods presented in this paper are useful for modeling TDI CCDs.

Keywords: time delay and integration charge coupled device, noise measurement, remote sensing application

PACS: 72.70.+m   **DOI:** 10.1088/1674-1056/20/8/087202

1. Introduction

The charge coupled device (CCD) was invented by Boyle and Smith in 1969.[1] Since it has the virtues of low noise, high dynamic range, high quantum efficiency, and wide spectral response, it has been widely used in general imaging, machine vision, and scientific and military applications.[2−6] The time delay and integration (TDI) mode of the CCD can provide increased sensitivity without sacrificing spatial resolution, and the effective integration time is increased by noise, which is equal to the number of the TDI stage, so TDI CCD plays a key role in a remote sensing system to improve the low light level capability.[7−9] For example, the most important payload of Chang'e II is the TDI CCD stereo camera with 96 stages. As illumination of the lunar surface is relatively low, the performance of Chang'e II's camera is characterized by the signal to noise ratio (SNR) of the TDI CCD mostly: the higher the SNR is, the more useful the information that can be extracted from the lunar surface images.

A number of reports on CCD noise models have been published. Holst[10,11] and Janesick[12] gave a thorough understanding of CCD noise sources and mathematical formulation. According to their analysis, Irie *et al.*[13] presented a technique to identify and measure the prominent sources of sensor noise in commercially available CCD video cameras by the analysis of the output images. Using physical models for CCD video cameras and material reflectance, Healey *et al.*[14] quantified the variation in digitized pixel values that was due to sensor noise and scene variation, and Chen[15] proposed a method by which noise was picked up from an image by a specially designed digital high-pass filter. However, this work was based purely on the frame CCD so it was not suitable for TDI CCD calibration. In addition, world leading TDI CCD suppliers, such as DALSA, Fairchild and E2V, only provided noise reports of TDI CCD in given conditions, where illumination, the TDI stage and line frequency are constant. As we all know, the elementary report is insufficient for the design of a remote sensing system, since the space environment is complex and volatile. From the above, we learn that there has been little work on the assessment and validation of TDI CCD noise by experimental evaluation, thus we have two objectives here. First, we will try to explore the relationship between noise models and TDI stages. Secondly, we wish to find a noise measurement method for TDI CCDs in particular.

http://www.iop.org/journals/cpb   *http://cpb.iphy.ac.cn*

2. Noise model of TDI CCD

Based on the model presented by Holst,[16] we show a CCD signal transfer diagram in Fig. 1. The equation of a video signal is expressed as

$$D = I + I \times R_{\mathrm{prnu}} + N_{\mathrm{ph}}(I) + N_{\mathrm{f}}$$
$$+ N_{\mathrm{dark}} + N_{\mathrm{read}} + N_{\mathrm{rst}} + N_{\mathrm{Q}}, \qquad (1)$$

where I is the sensor irradiance, $N_{\mathrm{ph}}(I)$ is the photo shot noise, N_{f} is the fixed pattern noise, N_{dark} is the dark current noise, N_{read} is the circuit readout noise, N_{rst} is the reset noise, N_{Q} is the quantization noise, R_{prnu} is the photo response non-uniformity ratio at a given TDI stage, and $I \times R_{\mathrm{prnu}}$ represents the photo response non-uniformity.
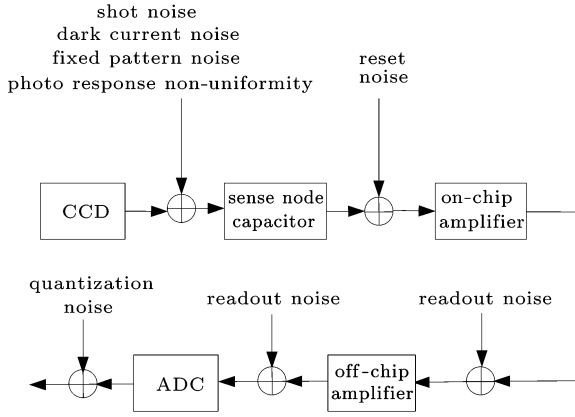

Fig. 1. The noise model of the TDI CCD.

From the viewpoint of noise properties, we divide CCD noises into three types: shot noise, pattern noise, and signal processing noise. The noise descriptions are summarized in Tables 1 to 3.

Table 1. Shot noise classification.

Noise type	Manifestation	Dependency
Photo shot noise	additive, temporal variance	incident illumination
Dark current shot noise	additive, temporal variance	temperature, exposure time

Table 2. Pattern noise classification.

Noise type	Manifestation	Dependency
Fixed pattern noise	additive, spatial variance	temperature, exposure time
Photo-response non-uniformity noise	multiplicative, spatial variance	incident illumination

Table 3. Signal processing noise classification.

Noise type	Manifestation	Dependency
Readout noise	additive, temporal variance	temperature, CCD readout rate
Reset noise	additive, temporal variance	temperature
Quantization noise	additive noise	variance of image

2.1. Shot noise versus TDI stage

Shot noise is a result of the quantum nature of light and characterizes the uncertainty in the number of electrons stored in a pixel. This number of electrons follows a Poisson distribution so that its variance equals its mean. Shot noise is a by-product and cannot be eliminated. It is important to note that any dark current contributing to the charge stored in a pixel will increase the mean and the variance in the number of electrons. The number of electrons (n_{e}) integrated in a pixel is given by

$$n_{\mathrm{e}} = n_{\mathrm{pe}} + n_{\mathrm{dc}}, \qquad (2)$$

where n_{pe} is the number of electrons generated by incident illumination, and n_{dc} is the number of electrons due to dark current.

A TDI CCD might produce n_{pe} at a pixel given by

$$n_{\mathrm{pe}} = t_{\mathrm{INT}} N_{\mathrm{TDI}} A_{\mathrm{D}} \int_{\lambda} B(\lambda) R_{\mathrm{E}}(\lambda) \mathrm{d}\lambda, \qquad (3)$$

where t_{INT} is the integration time for one stage, N_{TDI} is the number of TDI stages, A_{D} is the pixel area, $B(\lambda)$ is the incident spectral irradiance, and $R_{\mathrm{E}}(\lambda)$ is defined as the ratio of electrons collected per incident light energy as a function of wavelength λ.

The number of thermally generated dark current electrons is

$$n_{\mathrm{dc}} = \frac{J_{\mathrm{D}} A_{\mathrm{D}} N_{\mathrm{TDI}} t_{\mathrm{INT}}}{q}, \qquad (4)$$

where J_{D} is the dark current density and q is the electron charge.

From Eq. (3) and Eq. (4), we see that the number of photo electrons and the number of dark current electrons both increase linearly with the number of the TDI stage. Meanwhile, the variance of the shot noise also increases linearly with the number of the TDI stage.

2.2. Pattern noise versus TDI stage

Pattern noise refers to the pixel to pixel variation that does not change significantly from frame to frame. The N_{f} is primarily due to dark current differences, while R_{prnu} is due to differences in responsivity when light is applied. As a camera sweeps over a line of pixels, the pixels collect charge. At certain intervals, a TDI sensor shifts its collected charge from one stage to the next in the same direction as the camera travels. The sensor exposes the line of pixels again, and shifts again. In the process of charge transfer and accumulation, pattern noise decreases as the TDI stages increase due to the fact that the multiple integration stage creates inherent averaging effects.

2.3. Signal processing noise versus TDI stage

Once the exposure of all stages is finished, the sensor transfers its aggregate charge to readout registers that feed each pixel's charge from the image sensor into an output node that converts it into voltages. After this transfer and conversion, the voltages are amplified to become the camera's analog outputs, and finally the analog to digital converter (ADC) converts the voltages to digital numbers. During the process of signal processing, reset noise, readout noise, and quantization noise are introduced. However, this process takes place only after charge transfers, it has nothing to do with the TDI stage, so we will focus on the relationship between shot noise, pattern noise, and the TDI stage.

3. Noise measurement method of TDI CCD

In this section, we will describe a method for the noise measurement of TDI CCD. Generalizing the individual pixel mode of Eq. (1), we describe the output of a digitized TDI CCD camera image by

$$
\begin{aligned}
D(i,j) = {} & I(i,j) + I(i,j) \times R_{\mathrm{prnu}} + N_{\mathrm{ph}}(I(i,j)) \\
& + N_{\mathrm{f}}(i,j) + N_{\mathrm{dark}}(i,j) + N_{\mathrm{read}}(i,j) \\
& + N_{\mathrm{rst}}(i,j) + N_{\mathrm{Q}}(i,j).
\end{aligned} \tag{5}
$$

3.1. Spatial noise estimation

Noting that averaging multiple lines of images reduces the temporal variance noise, while it enhances the spatial variance noises, we can estimate the fixed pattern component of the i-th pixel by

$$
\hat{N}_{\mathrm{S}}(i) = \frac{1}{N} \sum_{j=1}^{N} D(i,j) - I, \tag{6}
$$

where $\hat{N}_{\mathrm{S}}(i)$ is a random variable with mean value of $N_{\mathrm{S}}(i)$ and a variance of σ_{T}^2/N, and N represents the exposure time of TDI CCD.

Then $\hat{N}_{\mathrm{S}}(i)$ can be written as

$$
\hat{N}_{\mathrm{S}}(i) = N_{\mathrm{S}}(i) + N_{\Delta T}(i), \tag{7}
$$

where $N_{\Delta T}(i)$ is a zero mean variable with variance of σ_{T}^2/N. Then we can estimate spatial noise by

$$
\hat{\sigma}_{\mathrm{S}}^2 = \frac{1}{M-1} \sum_{j=1}^{M} \hat{N}_{\mathrm{S}}^2(j). \tag{8}
$$

3.2. Temporal noise estimation

We can estimate temporal noise introduced in the i-th pixel by

$$
\hat{\sigma}_{\mathrm{T}}^2(i) = \frac{1}{N-1} \sum_{j=1}^{N} D(i,j)^2. \tag{9}
$$

The temporal noise of each pixel contributes to the entire quantity of noise. M represents the resolution of the TDI CCD. So σ_{T}^2 can be estimated by

$$
\hat{\sigma}_{\mathrm{T}}^2 = \frac{1}{M} \left(\sum_{i}^{N} \hat{\sigma}_{\mathrm{T}}^2(i) \right). \tag{10}
$$

4. Experimental system and evaluation of estimated results

Figure 2 shows a block diagram of the measurement system, where an integrating sphere is used to provide even illumination, and its illumination intensity is adjustable. The integrating sphere is positioned in front of the camera, and the captured images are downloaded to the host computer through a camera link cable and corresponding frame grabber. The practical measurement system was performed at the ambient temperature of 22 °C approximately, and the TDI CCD temperature was 30 °C approximately.

Thus this ensures that temperature-dependent noise will remain stable during the measurement procedure.
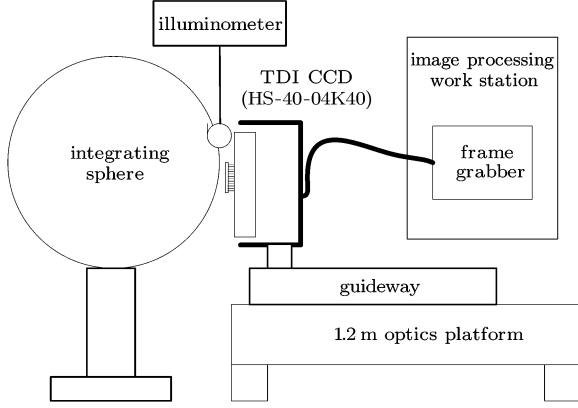

Fig. 2. Block diagram of measurement system.

We choose a HS-40-04K40 TDI CCD as the camera in the experiment.[17] Details of the CCD are listed in Table 4.

Table 4. HS-40-04K40 camera features.

Parameter	Value
Native resolution	4096
Full well capacity/e$^-$	90000
Dynamic range	313
TDI stage selection	16, 32, 48, 64, 80, 96
Camera output resolution/bits	12
Camera line rate/kHz	20
Analog gain/dB	0
Digital gain/dB	0

4.1. Fixed pattern noise measurement

Fixed pattern noise is measured by analysing a set of images taken in the dark environment without illumination. Then equation (1) becomes

$$D_{\text{dark}} = N_{\text{f}} + N_{\text{dark}} + N_{\text{read}} + N_{\text{rst}} + N_{\text{Q}}. \quad (11)$$

The temporal averaging of the image will effectively remove the terms N_{dark}, N_{read}, N_{rst}, and N_{Q}, and leave the component of N_{f} alone. We illustrate the measured N_{f} in Fig. 3.

As N_{f} is a function of temperature and exposure time, both of which are stable during the test proce-
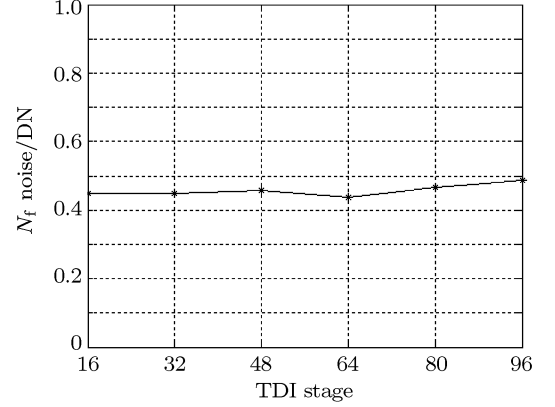
dure, it has no relationship with the TDI stage.

Fig. 3. Measured fixed pattern noise versus TDI stage.

4.2. Evaluation of quantization noise

To generate a digital image that can be stored in a computer, the analog signal from the camera is quantized by using an ADC. It is common for images to be quantized from 8 to 16 bits. Usually the quantization step is very small in comparison with the noise floor of the TDI CCD such that noise added in the quantization process becomes negligible.[18] The quantization noise is a zero mean random variable that is independent of the video signal with a uniform probability distribution over the range $[-q/2, \; q/2]$, where q is the quantization step and its variance is given by

$$N_{\text{Q}}^2 = \frac{q^2}{12}. \quad (12)$$

4.3. Measurement of readout noise, dark current shot noise, and reset noise

Readout noise, dark current shot noise, and reset noise are given by

$$D_{\text{dark,t}} = N_{\text{read}} + N_{\text{dark}} + N_{\text{rst}} + N_{\text{Q}}, \quad (13)$$

where $D_{\text{dark,t}}$ is temporal noise without illumination. Subtracting N_{Q} gives $N_{\text{read}} + N_{\text{dark}} + N_{\text{rst}}$. Since the reset noise will be reduced to a negligible level using correlated double sampling technology, we only focus on the readout noise and the dark current shot noise. We know that N_{dark} is a function of the TDI stage, so the value of N_{read} can be determined by extrapolation to zero of the temporal noise curve. However, as figure 4 shows, the shape of the $N_{\text{read}} + N_{\text{dark}} + N_{\text{rst}}$ noise curves is effectively flat, showing no apparent

trend of increase as the TDI stage increases. This phenomenon indicates that N_{dark} is swamped by read-out noise, therefore it is sufficient to consider readout noise alone in most cases.
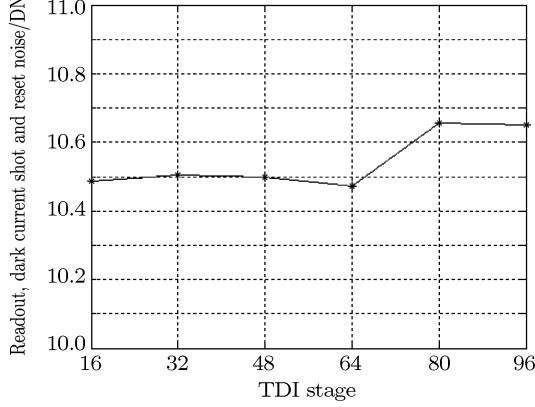

Fig. 4. Measured readout noise, dark current shot noise, and reset noise versus TDI stage.

4.4. Measurement of photo shot noise

For a given illumination, we could remove the spatial noise terms N_{f} and R_{prnu}, and then equation (1) becomes

$$D_{\text{t}} = I + N_{\text{ph}}(I) + N_{\text{dark}} + N_{\text{read}} + N_{\text{rst}} + N_{\text{Q}}. \quad (14)$$

Photo shot noise can be measured by subtracting I, then subtracting the previously measured $N_{\text{dark}} + N_{\text{read}} + N_{\text{rst}}$ and N_{Q}. Figure 5 shows the photo shot noise captured at all available TDI stages with different illumination intensities.
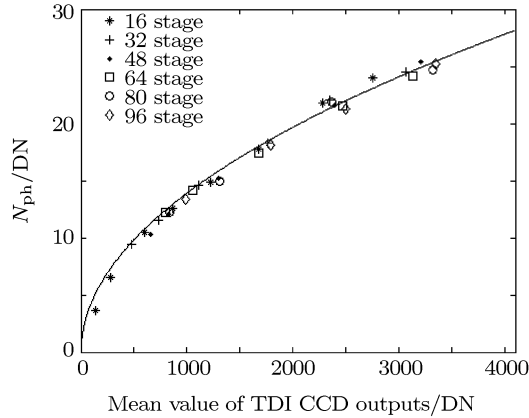

Fig. 5. Measured photo shot noise versus TDI stage.

4.5. Measurement of photo response non-uniformity noise

Using the measurement method presented in Subsection 3.1, we remove temporal terms from Eq. (1), and the value for spatial noise is given by

$$D_{\text{s}} = I + I \times R_{\text{prnu}} + N_{\text{f}}. \quad (15)$$

The amplitude of R_{prnu} noise for a particular irradiance can be calculated by subtracting I and N_{f}. Then we illustrate the measured R_{prnu} noise for all TDI stages. From Fig. 6 we find that R_{prnu} noise increases approximately linearly with I for a given TDI stage.
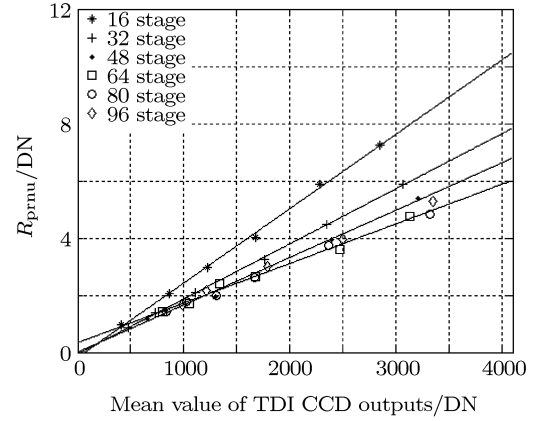

Fig. 6. Measured photo response non-uniformity noise versus TDI stage.

The R_{prnu} noise for particular TDI stages is defined as the best-fit line,

$$R_{\text{prnu16}} = 0.0026I - 0.1815,$$
$$R_{\text{prnu32}} = 0.0019I - 0.0630,$$
$$R_{\text{prnu48}} = 0.0017I + 0.0012,$$
$$R_{\text{prnu64}} = 0.0014I + 0.3347,$$
$$R_{\text{prnu80}} = 0.0014I + 0.2843,$$
$$R_{\text{prnu96}} = 0.0015I + 0.2698. \quad (16)$$

According to the description in Subsection 2.2, we summarize the non-uniformity ratio obtained in Table 5. This indicates that our experimental results match the theoretical analysis well.

Table 5. Comparison of non-uniformity ratio.

TDI stage	16	32	48	64	80	96
Non-uniformity ratio	0.0026	0.0018∼0.0026	0.0015∼0.0026	0.0013∼0.0026	0.0011∼0.0026	0.0010∼0.0026
Measured non-uniformity ratio	0.0026	0.0019	0.0017	0.0014	0.0014	0.0015

5. Conclusion

The TDI CCD plays an important role in remote sensing systems. In this paper, the noise components of the TDI CCD are grouped into three main types: shot noise, pattern noise, and signal processing effect noise. We elaborate the influence on these three noise models caused by TDI operation mode. A technique for measuring noise has also been developed. The derived TDI CCD noise model was tested by using a standard device at the National Supervisor & Test Centre for Optics and Mechanics Quality. The model response compares favourably with measured total image noise. So far this technique has been used in the design and evaluation of practical aerial TDI CCD cameras successfully, and more than 40 devices have been calibrated with it. All of the calibrated TDI CCDs perform well in their special applications.

References

[1] Boyle W S and Smith G E 1970 *Bell Systems Technical Journal* **49** 585
[2] Wang D J, Zhang T and Kuang H P 2011 *Opt. Express* **19** 4868
[3] Ma T B, Guo Y F and Li Y 2010 *Opt. Precis. Eng.* **18** 2028 (in Chinese)
[4] Zhang X, Zheng Y G and Zhang H J 2006 *Chin. Phys.* **15** 2185
[5] Zhang L, Sun Z Y and Jin G 2011 *Opt. Precis. Eng.* **19** 641 (in Chinese)
[6] Du H D, Huang S X and Shi H Q 2008 *Acta Phys. Sin.* **57** 7685 (in Chinese)
[7] Li Z, Wei E B and Tian J W 2007 *Acta Phys. Sin.* **56** 3028 (in Chinese)
[8] Zonios G 2010 *Appl. Opt.* **49** 163
[9] Qu H S, Zhang Y and Jin G 2010 *Opt. Precis. Eng.* **18** 1896 (in Chinese)
[10] Holst G C 2008 *Electro-Optical Imaging System Performance* (Bellingham: SPIE Optical Engineering Press) p. 123
[11] Holst G C 2007 *CMOS/CCD Sensors and Camera Systems* (Bellingham: SPIE Optical Engineering Press) p. 47
[12] Janesick J R 2000 *Scientific Charge-Coupled Devices* (Bellingham: SPIE Optical Engineering Press) p. 214
[13] Irie K, McKinnon A E, Unsworth K and Woodhead I M 2008 *IEEE Trans. Circuits and Systems for Video Technology* **18** 280
[14] Healey G E and Kondepudy R 1994 *IEEE Trans. Pattern Anal. Mach. Intel.* **16** 267
[15] Chen L, Zhang X, Lin J and Sha D 2009 *Opt. Laser Technol.* **41** 574
[16] Holst G C 1998 *CCD Arrays, Cameras, and Displays* (Bellingham: SPIE Optical Engineering Press) p. 312
[17] Zheng G F, Zhang K and Han S L 2010 *Opt. Precis. Eng.* **18** 623 (in Chinese)
[18] Oppenheim A V and Schafer R W 2009 *Discrete-Time Signal Processing* (New York: Prentice Hall Press) p. 345